PLOS PATHOGENS

RESEARCH ARTICLE

Epithelium intrinsic vitamin A signaling co-ordinates pathogen clearance in the gut via IL-18

Namrata Iyer[1], Mayara Grizotte-Lake[1], Kellyanne Duncan[1], Sarah R. Gordon[2], Ana C. S. Palmer[1], Crystle Calvin[1], Guo Zhong[3], Nina Isoherranen[3], Shipra Vaishnava[1]*

1 Department of Molecular Microbiology and Immunology, Brown University, Providence, RI, United States of America, **2** Department of Molecular Biology, Cell Biology and Biochemistry, Brown University, Providence, RI, United States of America, **3** Department of Pharmaceutics, University of Washington, Seattle, WA, United States of America

* shipra_vaishnava@brown.edu

Citation: Iyer N, Grizotte-Lake M, Duncan K, Gordon SR, Palmer ACS, Calvin C, et al. (2020) Epithelium intrinsic vitamin A signaling co-ordinates pathogen clearance in the gut via IL-18. PLoS Pathog 16(4): e1008360. https://doi.org/10.1371/journal.ppat.1008360

Editor: Igor Eric Brodsky, University of Pennsylvania, UNITED STATES

Received: June 4, 2019

Accepted: January 27, 2020

Published: April 24, 2020

Data Availability Statement: All relevant data are within the manuscript and its Supporting Information files.

Funding: This work was supported by Brown University OVPR Research Seed Fund Award (GR300113) to N.I., NIH award (P20GM10903 and 1R01DK113265) to S.V. and CCFA career development award to S.V. The funders had no role in study design, data collection and analysis, decision to publish, or preparation of the manuscript.

Abstract

Intestinal epithelial cells (IECs) are at the forefront of host-pathogen interactions, coordinating a cascade of immune responses to protect against pathogens. Here we show that IEC-intrinsic vitamin A signaling restricts pathogen invasion early in the infection and subsequently activates immune cells to promote pathogen clearance. Mice blocked for retinoic acid receptor (RAR) signaling selectively in IECs (stop$^{\Delta IEC}$) showed higher *Salmonella* burden in colonic tissues early in the infection that associated with higher luminal and systemic loads of the pathogen at later stages. Higher pathogen burden in stop$^{\Delta IEC}$ mice correlated with attenuated mucosal interferon gamma (IFNγ) production by underlying immune cells. We found that, at homeostasis, the intestinal epithelium of stop$^{\Delta IEC}$ mice produced significantly lower amounts of interleukin 18 (IL-18), a potent inducer of IFNγ. Regulation of IL-18 by vitamin A was also observed in a dietary model of vitamin A supplementation. IL-18 reconstitution in stop$^{\Delta IEC}$ mice restored resistance to *Salmonella* by promoting epithelial cell shedding to eliminate infected cells and limit pathogen invasion early in infection. Further, IL-18 augmented IFNγ production by underlying immune cells to restrict pathogen burden and systemic spread. Our work uncovers a critical role for vitamin A in coordinating a biphasic immune response to *Salmonella* infection by regulating IL-18 production by IECs.

Author summary

Epithelial cells line the intestinal lumen, forming a barrier between the body and dietary and microbial contents in the lumen. Apart from absorbing nutrients from diet, these epithelial cells help mediate a stable, symbiotic relationship between commensal bacteria and the immune cells. During infection, they help co-ordinate the immune response to counter the infection. How dietary micronutrients, such as vitamin A, inform epithelial cell function during infection is poorly understood. Using a model where epithelial cells in the gut cannot respond to vitamin A signals, we find that epithelial vitamin A signaling

Competing interests: The authors have declared that no competing interests exist.

promotes resistance to *Salmonella* infection. We show that, vitamin A increases the production of a key cytokine, interleukin 18, by epithelial cells. IL-18 promotes shedding of infected epithelial cells to reduce the pathogen invasion while also inducing the production of interferon gamma by immune cells to mediate pathogen clearance. Thus, epithelial cells dynamically respond to dietary vitamin A to regulate interleukin 18 production and potentiate resistance to infection.

Introduction

Resistance to an invasive pathogen involves coordination between the early and late phase of the immune response to achieve pathogen clearance without excess collateral damage to the host. The intestinal epithelium is at the forefront of host-microbial interactions and is critical for orchestrating these immune responses during infection. Chemokines secreted by the epithelium are responsible for immune cell recruitment and activation [1]. T cells, NK cells as well as neutrophils are recruited to the colon during infection. They secrete pro-inflammatory cytokines such as interferon gamma (IFNγ) to promote bacterial clearance and halt systemic spread of the infection [2, 3]. Moreover, the epithelium itself undergoes cell shedding in the early stages of infection as an innate defense mechanism to clear intracellular pathogens [4, 5]. Mechanisms that orchestrate such diverse functions of intestinal epithelial cells (IECs) during an infection remain poorly studied.

Vitamin A is an important dietary nutrient. It is absorbed in the form of carotenoids and retinyl esters by intestinal epithelial cells and metabolized into its active form retinoic acid (RA). Retinoic acid receptor (RAR) and retinoid X receptor (RXR) form a nuclear complex that is activated by RA binding to induce target gene expression [6]. Retinoic acid signaling affects both the recruitment as well as activity of dendritic cells [7], T cells [8], B cells [9] and innate lymphoid cells (ILCs) [10] in the gut. The retinoic acid synthesized by epithelial cells, while available to underlying immune cells, is also capable of initiating a signaling response within IECs themselves. Retinoic acid signaling in intestinal epithelial cells regulates epithelial lineage specification and promotes small intestinal T helper 17 (Th17) responses [11, 12]. Dietary vitamin A deficiency markedly increases susceptibility to enteric pathogens [13], however, relatively little is known about the contribution of IEC-intrinsic retinoic acid signaling in the context of infection.

In this study we use a mouse model expressing dominant negative retinoic acid receptor ($stop^{\Delta IEC}$) in IECs to investigate the role of retinoic acid signaling during infection. $stop^{\Delta IEC}$ mice are more susceptible to luminal and systemic colonization by *Salmonella*. This is associated with abrogated shedding of infected epithelial cells as well as a blunted interferon gamma (IFNγ) response. We find that expression of interleukin-18, a known inducer of IFNγ, is dependent on retinoic acid signaling in intestinal epithelial cells. RAR signaling-dependent IL-18 promotes epithelial cell shedding as well as mucosal IFNγ production to orchestrate resistance to infection. Our results thus reveal a novel regulatory axis in the gut, wherein epithelial-intrinsic signaling in response to vitamin A, sequentially triggers IL-18 dependent mechanisms to first limit tissue invasion and then trigger an IFNγ response to promote pathogen clearance.

Results

Epithelial-intrinsic RAR signaling is protective against *Salmonella* colonization

Vitamin A deficiency results in increased susceptibility to infection by *Salmonella* and other enteric pathogens [13, 14]. Vitamin A deficiency causes immune dysregulation in the gut,

including improper lymphoid recruitment, maturation and functional potential [15, 16]. These sweeping changes obscure the finer details of how vitamin A regulates infection outcome. Dietary vitamin A is sequentially absorbed, metabolized and distributed by intestinal epithelial cells [17]. Retinoic acid synthesized by intestinal epithelial cells regulates immune cell recruitment and cytokine production [18, 19]. We hypothesized that vitamin A signaling in IECs regulates the mucosal immune response to mediate infection susceptibility. To address this question, we chose a mouse model wherein vitamin A signaling was specifically abrogated in intestinal epithelial cells downstream of metabolism of vitamin A. Retinoic acid receptor alpha was found to be the most dominant RAR isoform expressed in intestinal epithelial cells (Fig 1A). Our mouse model used a Villin-Cre dependent overexpression of a dominant negative form of retinoic acid receptor alpha (Fig 1B) [20, 21]. Intestinal epithelial cells in these mice ($stop^{\Delta IEC}$) were defective in the expression of the RA-responsive gene *isx* compared to their wild type littermates ($stop^{flox}$) (Fig 1C) [22]. To assess if disrupting RA signaling in IECs influenced retinoid metabolism we carried out quantification of total retinoids in the colon tissues of $stop^{flox}$ and $stop^{\Delta IEC}$ mice. Abrogation of RAR signaling in the epithelium did not have any effect on intestinal vitamin A sufficiency. $stop^{\Delta IEC}$ mice displayed heightened levels of tissue retinoic acid and retinyl esters suggesting compensatory mechanisms to maintain vitamin A sufficiency in the tissues (S1A Fig). RA signaling is known to be involved in IEC proliferation and differentiation. We saw that at homeostasis, $stop^{\Delta IEC}$ mice displayed an increase in goblet cell differentiation as well as overall thickness of the mucus barrier (S1B and S1C Fig), corroborating the results of a previous study using $RAR\alpha^{\Delta IEC}$ mice [11]. However, $stop^{\Delta IEC}$ mice showed no significant differences in epithelial turnover (S1D and S1E Fig).

The role of epithelial-intrinsic vitamin A signaling during infection was assessed using a gastroenteritis infection model of non-typhoidal *Salmonella* Typhimurium (Fig 1D) [23]. Bacterial burden was determined at early (18 hours post infection; hpi) and late (72 hpi) time points to assess if vitamin A signaling modulates the kinetics of the pathogen colonization. At early time points, $stop^{\Delta IEC}$ mice and $stop^{flox}$ littermate controls had similar luminal burdens of the pathogen. However, $stop^{\Delta IEC}$ mice showed significantly higher loads of the bacterium within colon tissues (Fig 1E). This advantage in initial tissue invasion bolstered pathogen burdens at later time points, with higher loads found in the feces, colon as well as mesenteric lymph nodes of $stop^{\Delta IEC}$ mice (Fig 1F). Retinoic acid receptor expression itself remained unchanged during infection (S1F Fig). In addition, infection outcome was independent of the microbiome as homeostatic fecal microbiome composition of $stop^{\Delta IEC}$ mice was similar to that of $stop^{flox}$ mice (S2A–S2C Fig). These results show that loss of RAR signaling in the intestinal epithelium phenocopies dietary vitamin A deficiency in the context of enteric infection. Further, the changes in infection kinetics suggest that epithelial-intrinsic vitamin A signaling co-ordinates early and late immune mechanisms to promote resistance to infection.

Epithelial-intrinsic RAR signaling promotes mucosal IFNγ response during infection

Vitamin A metabolism and signaling in the epithelium are key determinants of the intestinal immune make up. In the gut, retinoic acid influences the balance between Th1 and Th17 cells, both of which are important for controlling infection [8, 24, 25]. IEC-intrinsic vitamin A metabolism promotes mucosal IL-22 production, which in turn induces dysbiosis and aids pathogen colonization [18]. We therefore analyzed the colonic lamina propria populations in our mouse model to check if the increased susceptibility of $stop^{\Delta IEC}$ mice is due to a dysregulated immune response. $stop^{\Delta IEC}$ and $stop^{flox}$ mice showed similar colonic immune make-up at homeostasis (S3A–S3D Fig). However, on day 3 of *Salmonella* infection, $stop^{\Delta IEC}$ mice

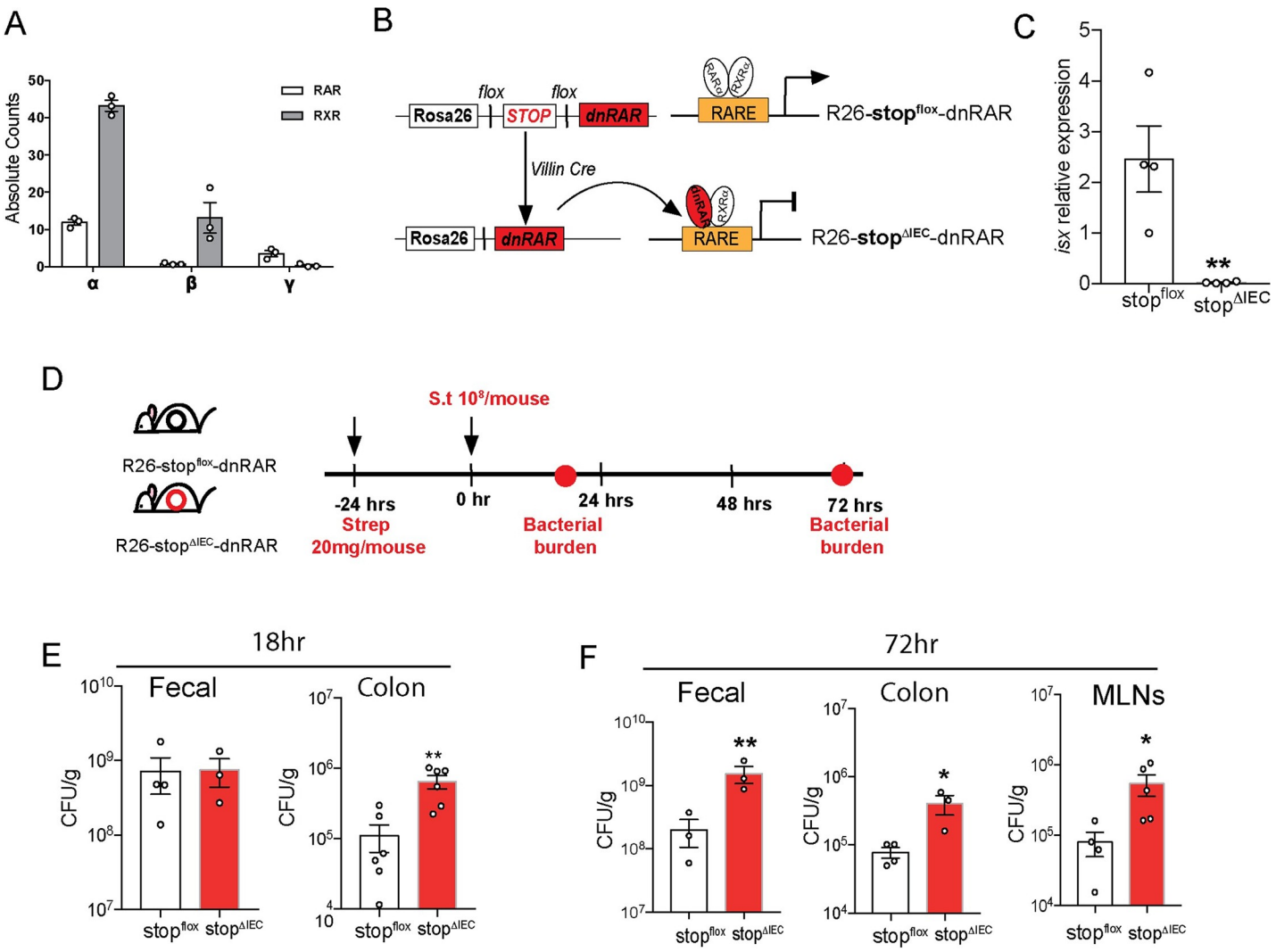

Fig 1. Epithelial-intrinsic RAR signaling is protective against *Salmonella* colonization. (A) Absolute counts of RAR and RXR isoforms (α, β and γ) in laser capture microdissected epithelial cells from homeostatic stop^{flox} mice ileal tissues **(B)** Schematic representation of the creation of stop^{flox} (wild type) and stop$^{\Delta IEC}$ (RAR signaling knockdown) mice using Villin-Cre dependent expression of the dnRAR cassette. **(C)** Relative expression of vitamin A responsive gene, *isx*, in stop^{flox} and stop$^{\Delta IEC}$ ileum tissues. **(D)** Schematic representation of *Salmonella* infection timeline with assessment of pathogen loads at 18 hours and 72 hours post infection (hpi). **(E)** Bacterial burden in fecal and proximal colon tissues at 18 hpi in stop^{flox} and stop$^{\Delta IEC}$ mice. **(F)** Bacterial burden in fecal, distal colon and mesenteric lymph node samples at 72 hpi in stop^{flox} and stop$^{\Delta IEC}$ mice. Representative data from 3 independent experiments. n = 3–4 mice per group. Student's t test was used for statistical analysis. $^{*}P<0.05$; $^{**}P<0.01$.

https://doi.org/10.1371/journal.ppat.1008360.g001

displayed a defect in interferon gamma production (Fig 2A). CD4 and CD8 T cells as well as neutrophils were recruited to the colon to similar extents in stop$^{\Delta IEC}$ and stop^{flox} mice (S4A and S4B Fig), yet activation of these cells to produce IFNγ was defective in stop$^{\Delta IEC}$ mice (Fig 2B–2D). No significant differences in mucosal IL-17 and IL-22 production were observed between stop$^{\Delta IEC}$ and stop^{flox} mice during infection (S4C and S4D Fig).

To assess if the defect in IFNγ production was responsible for the increased susceptibility in stop$^{\Delta IEC}$ mice, we performed IFNγ feedback experiments (Fig 3A). Reconstitution of IFNγ in stop$^{\Delta IEC}$ mice led to a rescue of susceptibility, with bacterial burdens returning to wild type levels (Fig 3B and 3C). Previous studies, both *in vitro* and *in vivo*, have shown that interferon gamma can be regulated by vitamin A, with retinoic acid promoting IFNγ production in

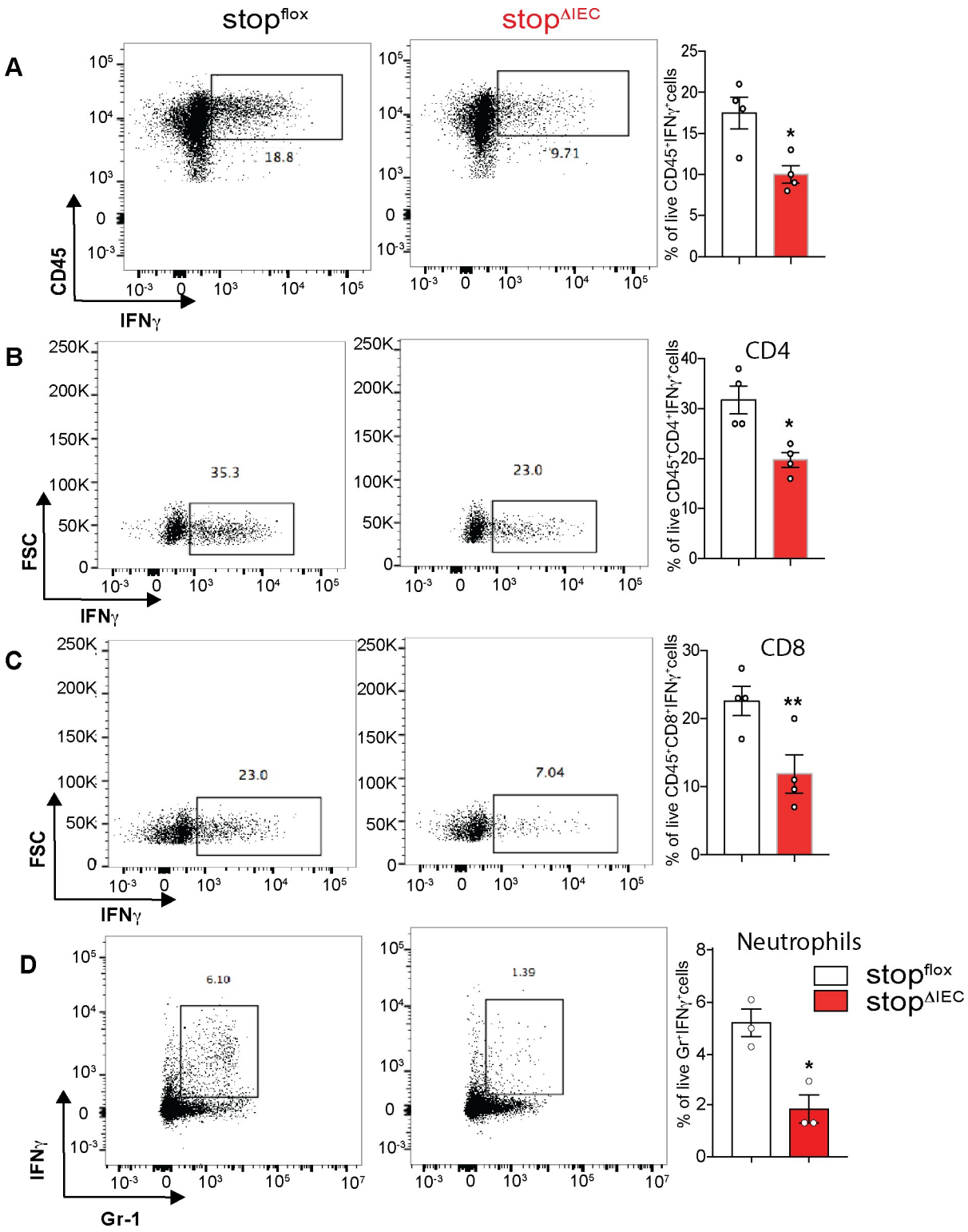

Fig 2. Epithelial-intrinsic RAR signaling promotes mucosal IFNγ response during infection. (A-D) Flow cytometry analysis of colonic lamina propria lymphocytes from stop^{flox} and stop$^{\Delta IEC}$ mice 72 hpi with *Salmonella*. Representative density plots and quantitative analysis of relative frequencies of **(A)** total live CD45+ IFNγ+ cells **(B)** CD4+ IFNγ+ cells **(C)** CD8+ IFNγ+ cells and **(D)** Gr-1+IFNγ+ cells in stop^{flox} and stop$^{\Delta IEC}$ mice. Representative data from 2 independent experiments. n = 3–4 mice per group. Student's t test was used for statistical analysis. $^{*}P<0.05$; $^{**}P<0.01$.

https://doi.org/10.1371/journal.ppat.1008360.g002

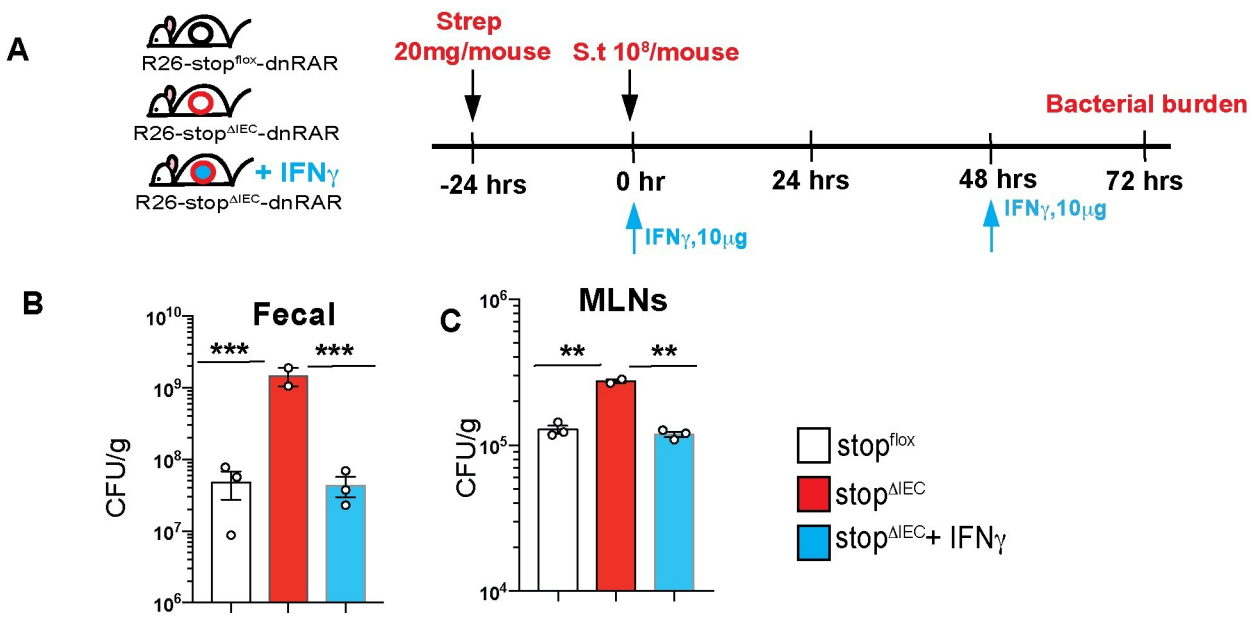

Fig 3. Epithelial RAR signaling promotes IFNγ response to mediate pathogen clearance. (A) Schematic representation of IFNγ feedback in stop$^{\Delta IEC}$ mice during *Salmonella* infection. Mice were intraperitoneally injected with 10 μg of IFNγ at 0 hpi and 48 hpi. Bacterial burden in **(B)** fecal and **(C)** mesenteric lymph nodes at 72 hrs post *Salmonella* infection in stop^{flox}, stop$^{\Delta IEC}$ and stop$^{\Delta IEC}$ + IFNγ mice. One-way ANOVA was used for statistical analysis. $^{**}P<0.01$, $^{***}P<0.005$.

https://doi.org/10.1371/journal.ppat.1008360.g003

intestinal T cells [26, 27]. Interferon gamma promotes resistance mechanisms such as phagocytosis to help restrict intestinal and systemic *Salmonella* infection [28, 29].Our results suggest that epithelial-intrinsic RAR signaling primes mucosal IFNγ production to restrict *Salmonella* infection.

Intestinal epithelium-intrinsic RAR signaling regulates interleukin-18

Interleukin-18 was first discovered as an interferon gamma inducing molecule [30, 31]. This IL-1 family cytokine is constitutively expressed by a wide variety of cell types in the body. In the gut, intestinal epithelial cells form the main source of IL-18 [32, 33]. We hypothesized that interleukin-18 might be the mechanistic link between IEC-intrinsic RAR signaling and mucosal IFNγ response. A previous study with human neuroblastoma cells identified induction of IL-18 by all trans retinoic acid *in vitro* [34]. Further, serum IL-18 levels have been shown to increase during vitamin A supplementation in obese mice [35]. However, regulation of homeostatic IL-18 levels in the gut by vitamin A has not been previously reported.

We assessed the levels of IL-18 at homeostasis between stop$^{\Delta IEC}$ and stop^{flox} mice. Colon whole tissue (Fig 4A) as well as colonocytes (Fig 4B) of stop$^{\Delta IEC}$ mice showed reduced protein levels of the precursor form of IL-18. In order to confirm that this phenomenon is not restricted to our stop$^{\Delta IEC}$ mouse model, we used a dietary model where wild type mice were fed a diet spiked with retinyl acetate for 2 weeks. Compared to mice receiving vehicle control, mice fed excess retinyl acetate had increased levels of IL-18 in colonocytes (Fig 4C). These results suggest that dietary vitamin A can dynamically modulate the levels of IL-18 in the colon.

Studies mining transcriptional targets of RAR signaling by *in silico* and ChIP-seq techniques have not identified IL-18 as a candidate, suggesting that retinoic acid receptor does not directly bind the *il18* promoter [36, 37]. In order to identify the mechanistic link between RAR

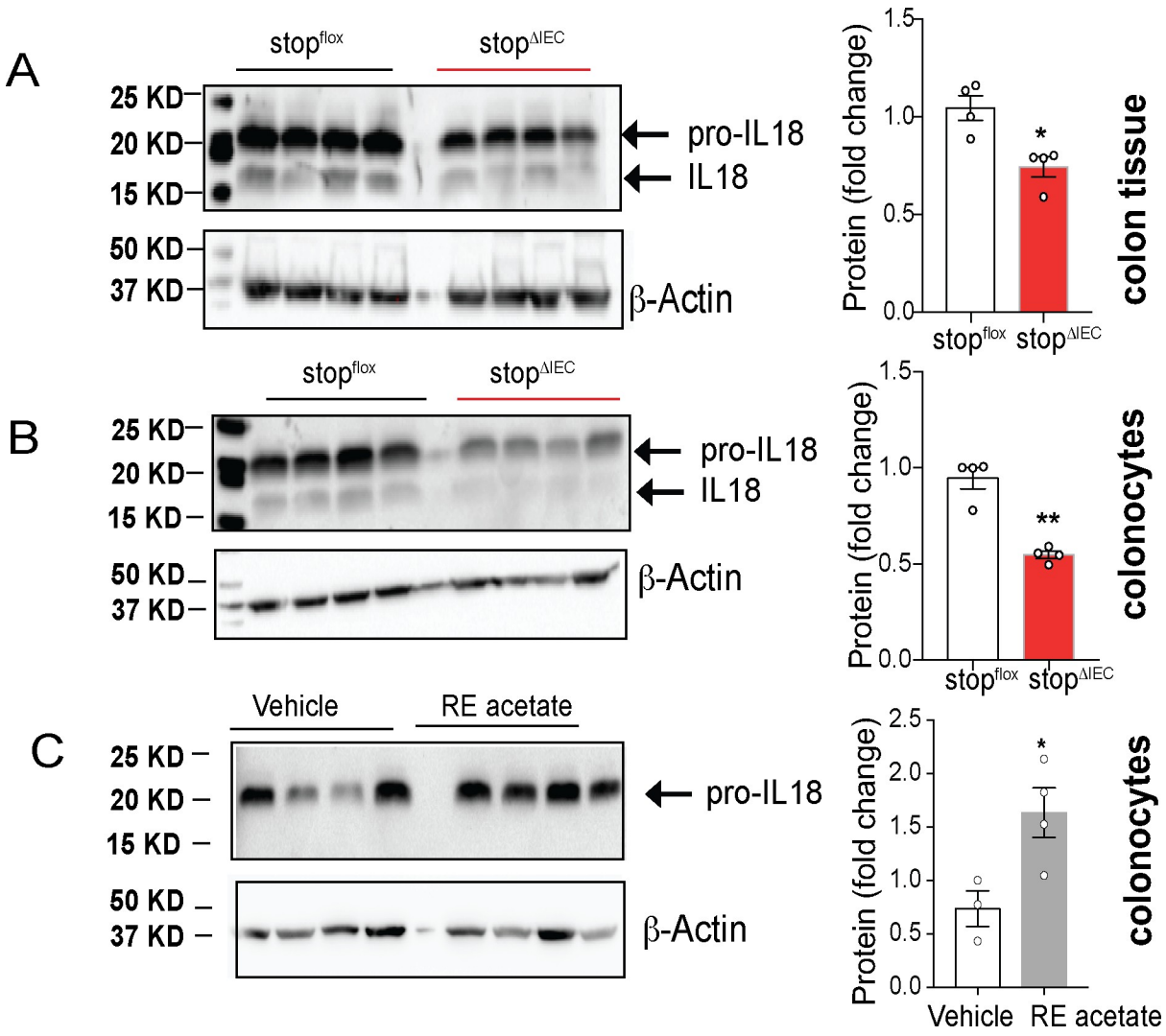

Fig 4. Intestinal epithelium-intrinsic RAR signaling regulates interleukin-18. Representative western blots and quantitative image analysis results comparing homeostatic levels of IL-18 in colon whole tissue **(A)** and colonocyte **(B)** lysates from stop^{flox} and stop$^{\Delta IEC}$ mice. Representative data from 2 independent experiments. **(C)** Representative western blot and quantitative image analysis comparing IL-18 levels in colonocytes from stop^{flox} mice fed regular mouse chow spiked with vehicle (corn oil) or retinyl acetate (500 IU/g) for 2 weeks. Representative data from 2 independent experiments. All quantitation analysis done for pro-IL18 levels in all experiments. ImageJ was used for densitometric analysis of image. β actin levels were used for normalization. Student's t test was used for statistical analysis. $^{*}P<0.05$; $^{**}P<0.01$.

https://doi.org/10.1371/journal.ppat.1008360.g004

signaling and IL-18, we performed RNAseq analysis on intestinal epithelial cells from stop$^{\Delta IEC}$ and stop^{flox} mice. RNAseq analysis confirmed that RAR signaling regulates *il-18* transcriptionally (S5A and S5B Fig). In our dataset, none of the known transcription regulators of IL-18 such as NF-κB, PU.1, Stat1, AP-1 and Bcl6 were differentially expressed in stop$^{\Delta IEC}$ mice [38–40]. One of the most upregulated genes in stop$^{\Delta IEC}$ mice was metallothionein-1 (*mt1*) (S5B and S5C Fig). Metallothioneins are intracellular zinc binding proteins that dynamically regulate the zinc available to other zinc-binding transcription factors [41–43]. The upregulation of *mt1* expression in stop$^{\Delta IEC}$ IECs correlated with a concomitant decrease in labile zinc levels quantified using the zinc reporter Zinpyr-1 (S5D and S5E Fig) [44]. Zinc is known modulate the activity of several transcription factors including AP1 and NF-κB and could be the link between RAR signaling and IL-18 [45].

RAR signaling-dependent IL-18 orchestrates early resistance to *Salmonella* invasion

Our results in stop$^{\Delta IEC}$ mice demonstrated a direct correlation between intestinal IL-18 levels, RAR signaling, IFNγ production and resistance to *Salmonella* infection. In order to unravel the causal relationship between IL-18, IFNγ and infection outcome, we reconstituted IL-18 and IFNγ in stop$^{\Delta IEC}$ mice and compared their susceptibility at early time points (18 hpi) of *Salmonella* infection. We found that while luminal colonization was unaffected, feedback with IFNγ failed to rescue early tissue invasion in stop$^{\Delta IEC}$ mice (Fig 5A–5C). On the other hand, IL-18 feedback in stop$^{\Delta IEC}$ mice rescued tissue burdens of the pathogen to levels comparable to stop^{flox} mice (Fig 5D–5F). This was further confirmed using confocal microscopy where staining for *Salmonella* revealed more bacteria within stop$^{\Delta IEC}$ colonic tissues compared to stop^{flox} and IL-18 feedback mice (Fig 5G–5I; S1–S3 Movies). Flow cytometry analysis at 18 hpi showed no significant changes in IFNγ production, corroborating the results obtained with IFNγ feedback at that timepoint (S6A and S6B Fig; Fig 5A–5C). These results indicate that epithelial RAR signaling promotes early resistance to bacterial invasion in an IL-18 dependent, but IFNγ independent, manner.

Early in the infection, *Salmonella* uses epithelial invasion as a strategy to induce tissue inflammation and gain a selective advantage over gut commensals [46, 47]. Recently, epithelial cell death has been identified as a strategy to eliminate infected cells in the gut and limit tissue colonization [48, 49]. In the context of infection, inflammasome-mediated cell death pathways and IL-18 secretion have been implicated in this epithelial-intrinsic response [4, 48, 50]. We hypothesized that RAR signaling in IECs modulates cell death response during *Salmonella* infection via IL-18. Cell death has been reported to occur as an early response to the infection, especially in the cecum which is more permissive to bacterial invasion [4]. We assessed the extent of cecal epithelial cell shedding in stop$^{\Delta IEC}$ mice at 18 hpi using cleaved caspase-3 staining as a marker for dying epithelial cells. We saw higher numbers of dying cells in stop^{flox} mice compared to stop$^{\Delta IEC}$ mice. This defect was rescued upon IL-18 reconstitution (Fig 5J–5M). In order to confirm the link between IL-18 and epithelial shedding, we performed neutralization experiments. Treatment of mice with IL-18 neutralizing antibody resulted in a concomitant decrease in cecal shedding during *Salmonella* infection (S7A–S7C Fig). This suggests that RAR signaling mediated IL-18 production promotes an epithelial cell shedding response which is associated with restricted tissue invasion by *Salmonella*.

Intestinal epithelium-intrinsic RAR signaling regulates pathogen colonization via interleukin-18

Our results with IFNγ feedback showed that at day 3 of infection, IFNγ is successfully able to rescue pathogen colonization in stop$^{\Delta IEC}$ mice (Fig 3A–3C). IL-18, but not IFNγ, feedback was required to rescue early tissue invasion susceptibility in stop$^{\Delta IEC}$ mice (Fig 5C and 5F). Therefore, we hypothesized that IL-18 levels in the gut promoted early innate defenses to infection, while priming mucosal IFNγ to mediate pathogen clearance in the later stages. We analyzed the effect of IL-18 reconstitution in stop$^{\Delta IEC}$ mice on day 3 of infection (Fig 6A). Feedback of IL-18 was sufficient to bring bacterial loads in fecal and MLN samples of stop$^{\Delta IEC}$ mice back to wild type levels (Fig 6B and 6C). Assessment of the colonic lamina propria showed that IL-18 feedback rescued IFNγ production by mucosal T cells (Fig 6D). These results suggest that epithelial RAR signaling modulates the mucosal IFNγ response via IL-18 to mediate resistance to pathogen. Our results align with a previous study where epithelial IL-18 expression, regulated by histone deacetylase 3 activity, primes IFNγ response in intraepithelial lymphocytes to restrict colonization by *Citrobacter* [51]. IL-18 induction by protozoan colonization in the gut

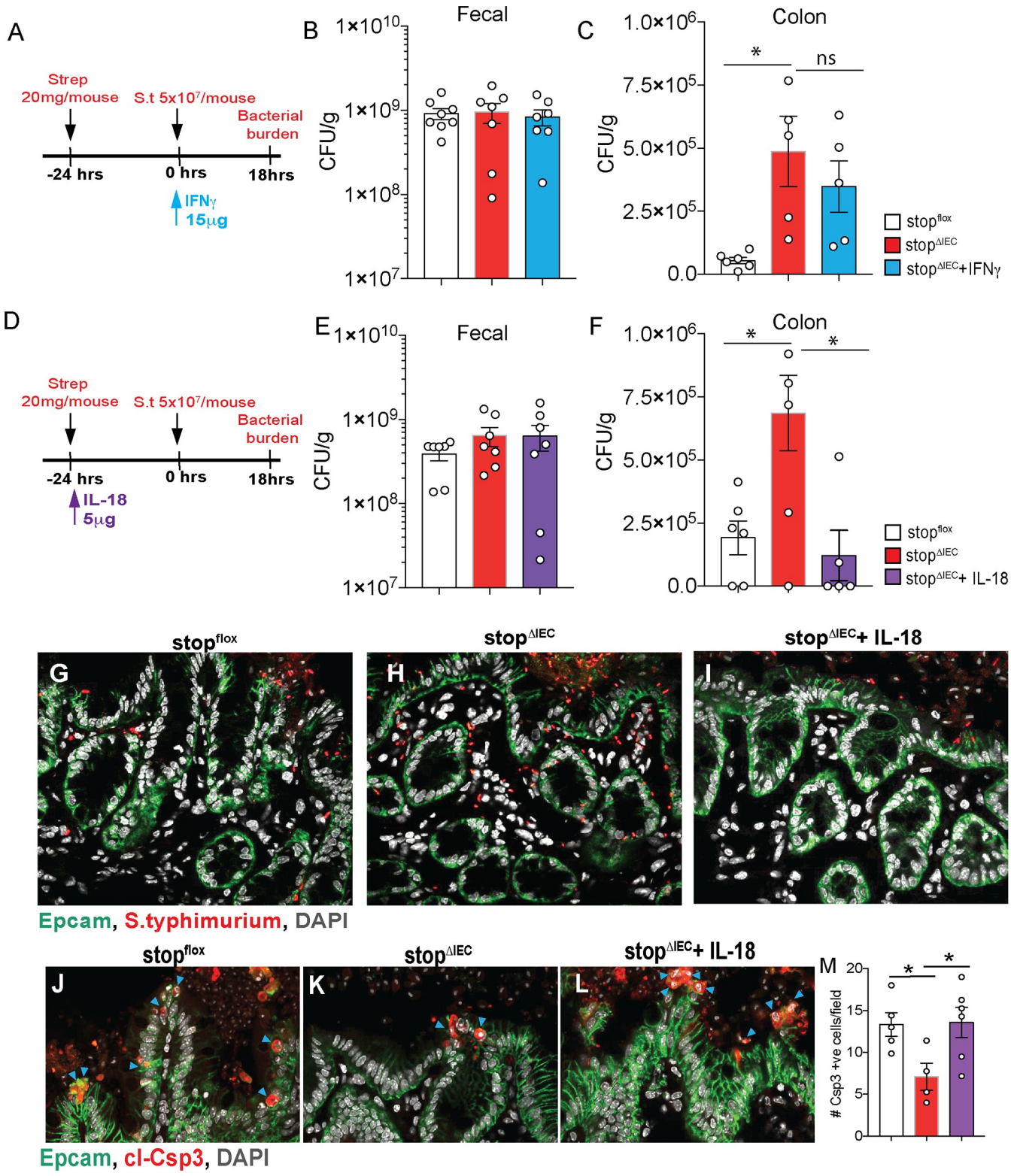

Fig 5. RAR signaling-dependent IL-18 orchestrates early resistance to *Salmonella* invasion. **(A)** Schematic representation of IFNγ feedback regimen for 18 hour time point in *Salmonella* infection. **(B)** Fecal and **(C)** Proximal colon bacterial loads at 18hpi in stop^{flox}, stop$^{\Delta IEC}$, and stop$^{\Delta IEC}$ + IFNγ mice. **(D)** Schematic representation of IL-18 feedback regimen for 18 hour time point in *Salmonella* infection. **(E)** Fecal and **(F)** Proximal colon bacterial loads at 18hpi in stop^{flox}, stop$^{\Delta IEC}$ and stop$^{\Delta IEC}$ + IL-18 mice. **(G, H and I)** Representative confocal microscopy images depicting loads of *Salmonella* (red) in colon tissue 18 hours post infection, counterstained with EpCAM (epithelial cells; green) and DAPI (nuclei; grey). **(J, K and L)** Representative images and **(M)** quantitative

analysis of epithelial cell death (cleaved caspase-3 positive cells; red) in cecal tissues of $stop^{flox}$, $stop^{\Delta IEC}$ and $stop^{\Delta IEC}$ + IL-18 mice at 18 hours post infection. Samples counterstained with Epcam (epithelial cells; green) and DAPI (nuclei; grey). Arrows indicate actively shedding Csp3 positive epithelial cells. Combined data from 2 independent experiments. Quantitative comparison was made by counting total Csp3+ve cells per image. Data is an average of 6–10 images per mouse with 3–4 mice per group per experiment. One-way ANOVA was used for statistical analysis. $^{*}P<0.05$; $^{**}P<0.01$, $^{***}P<0.005$.

https://doi.org/10.1371/journal.ppat.1008360.g005

protects against *Salmonella* by promoting mucosal Th1 and Th17 response [52]. Our results corroborate the importance of IL-18 as a determinant of infection susceptibility and reveal a previously unappreciated pathway for IL-18 regulation via vitamin A signaling and dietary vitamin A.

Discussion

Vitamin A is a potent dietary micronutrient and vitamin A deficiency causes susceptibility to a spectrum of infectious diseases. A large body of work has contributed to our understanding of the immunomodulatory potential of vitamin A and its metabolite retinoic acid. However, complex metabolic and distribution pathways as well as source- and concentration- dependent functional effects have made dietary vitamin A models difficult to interpret [53]. In this study, we employ a tissue-specific signaling abrogation model to elucidate the role of the vitamin A signaling pathway in the intestinal epithelium during infection. This model has no direct interference with the vitamin A metabolic machinery, avoiding any differences in gut immune trafficking. Specifically, this study extends our understanding of homeostatic functions of vitamin A signaling in the intestine and reveals a previously unappreciated regulatory role for this

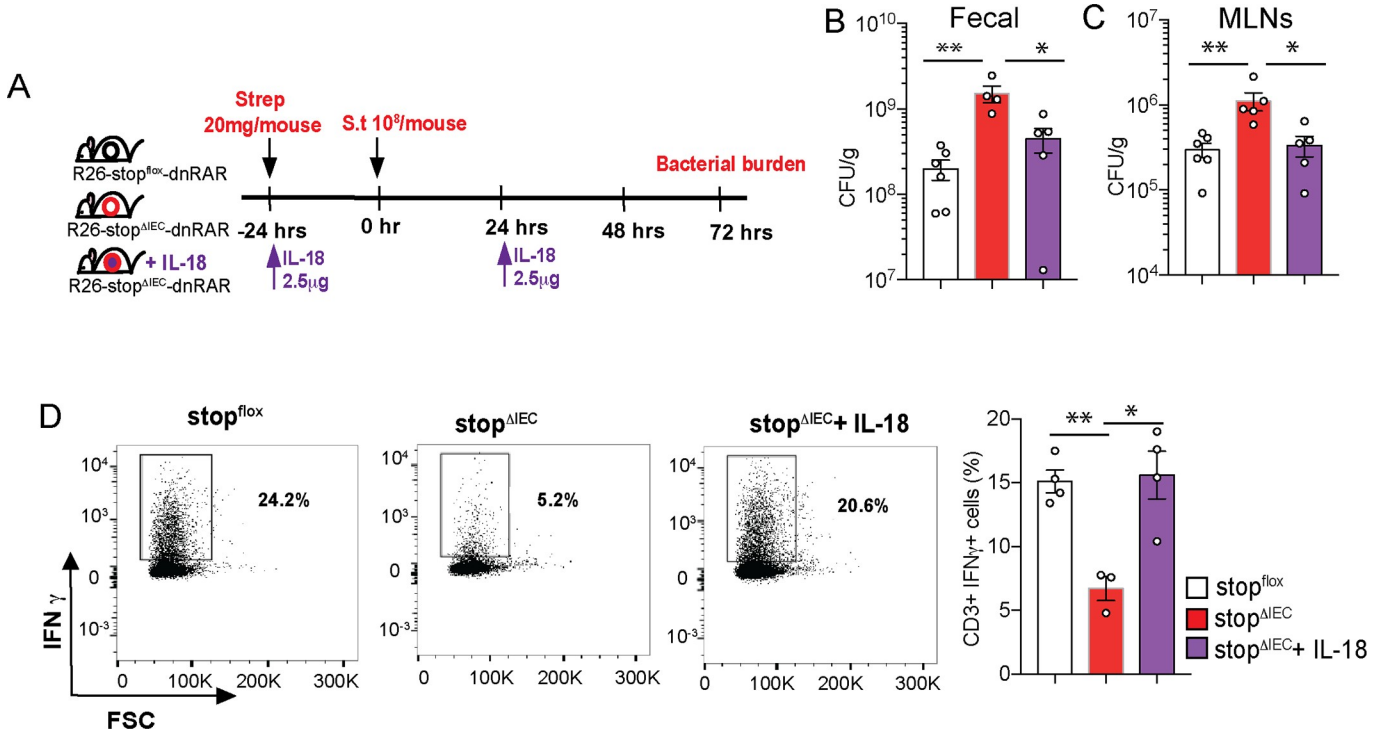

Fig 6. Intestinal epithelium-intrinsic RAR signaling regulates pathogen colonization via interleukin-18. (A) Schematic representation of IL-18 feedback regimen in $stop^{\Delta IEC}$ mice during *Salmonella* infection at 72 hpi. Bacterial burden in fecal **(B)** and mesenteric lymph nodes **(C)** at 72 hpi in $stop^{flox}$, $stop^{\Delta IEC}$ and $stop^{\Delta IEC}$ + IL-18 mice. Combined data from 2 independent experiments. **(D)** Flow cytometry analysis of colonic lamina propria lymphocytes from $stop^{flox}$, $stop^{\Delta IEC}$ and $stop^{\Delta IEC}$ + IL-18 mice with density plots and quantitative analysis of relative frequencies of CD3+IFNγ+ cells. Representative data from 2 independent experiments. n = 3–4 mice per group. One-way ANOVA was used for statistical analysis. $^{*}P<0.05$; $^{**}P<0.01$.

https://doi.org/10.1371/journal.ppat.1008360.g006

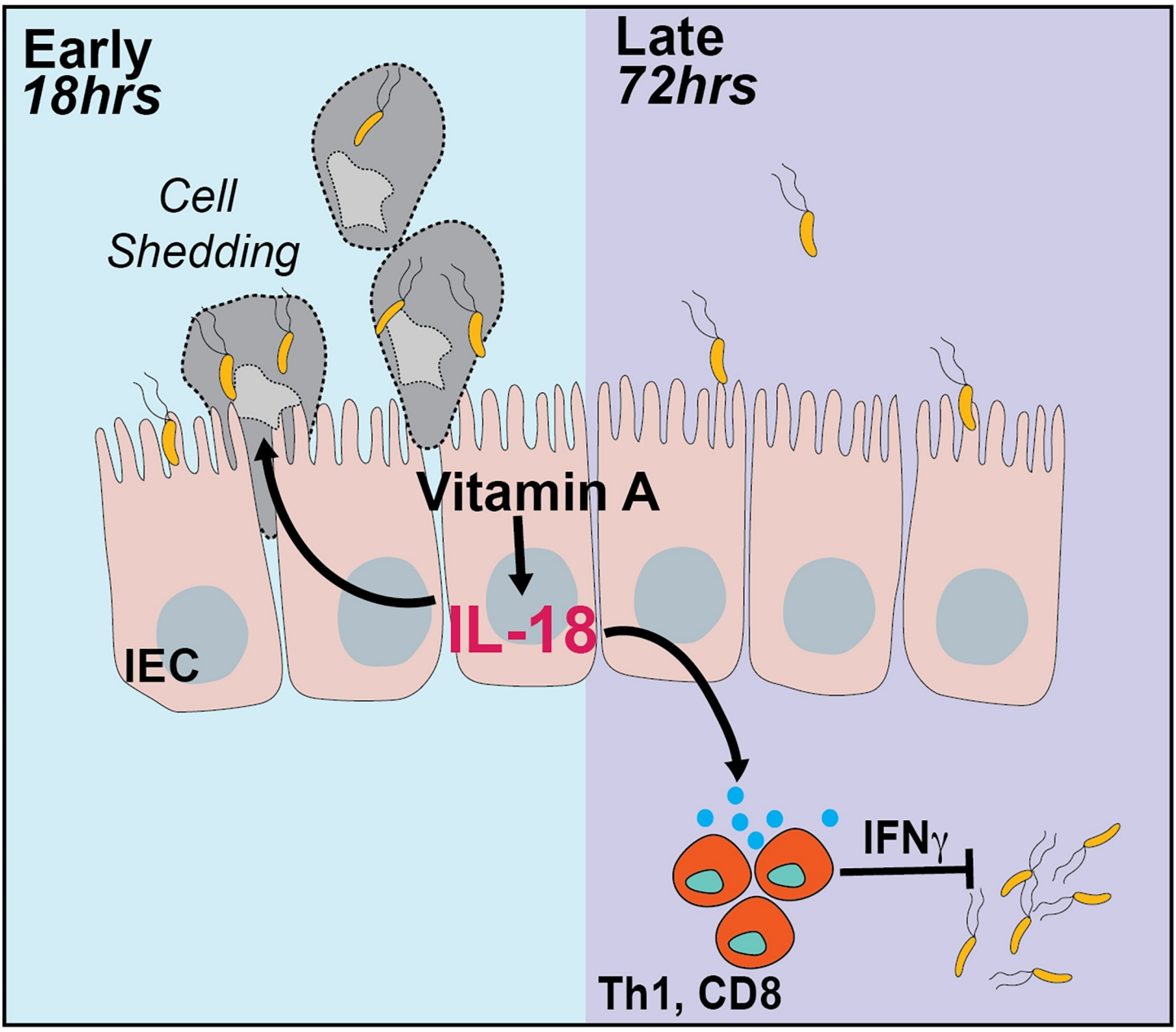

Fig 7. Model depicting role of epithelial-intrinsic signaling during *Salmonella* infection. Dietary vitamin A activates retinoic acid signaling within colonic epithelial cells to induce production of IL-18 at homeostasis. During early stages of *Salmonella* infection (18 hours), IL-18 promotes epithelial cell shedding to eliminate infected cells and restrict pathogen invasion. IL-18 also primes IFNγ production by mucosal immune cells which promote pathogen clearance during later stages of the infection (72 hours).

https://doi.org/10.1371/journal.ppat.1008360.g007

pathway during *Salmonella* infection. We describe the dynamic regulation of homeostatic IL-18 levels in the gut by vitamin A. We elucidate the functional role of the vitamin A-IL18 axis in restricting early tissue invasion by *Salmonella* and priming mucosal IFNγ production to mediate pathogen clearance (Fig 7).

Cytokines secreted by epithelial cells are important for immune co-ordination in the gut. Vitamin A is known to induce the signaling of important cytokines such as IL-22 in the gut [26]. A previous study from our group has shown that epithelial-intrinsic retinoic acid

synthesis promotes IL-22 expression in immune cells which in turn promotes *Salmonella* induced dysbiosis and gut colonization [18]. In contrast, the current study shows that epithelial-intrinsic RA signaling regulates IL-18 expression which protects against pathogen colonization and systemic spread. This highlights that retinoic acid synthesized by epithelial cells has distinct autocrine and paracrine functions, each having differential effects on infection outcome.

Interleukin-18 is set apart from other members of the IL-1 family by being constitutively expressed by wide range of cell types throughout the body [54]. TLR ligands (LPS, poly (I:C), pam3CSK4) and type I interferons induce expression of IL-18, which is then proteolytically processed via the inflammasome pathway [39]. While induction of IL-18 during inflammatory conditions is well documented, relatively little is known about homeostatic regulators of IL-18. Studies have shown that late in gestation, inactive IL-18 starts accumulating in the intestine and active IL-18 is detectable postnatally [55]. Microbial colonization of the gut induces an upregulation in IL-18 expression [56] and the microbial metabolite butyrate is implicated in transcriptional regulation of IL-18 [57]. This study is the first to demonstrate that homeostatic IL-18 levels in the gut are regulated by IEC-intrinsic vitamin A signaling. Further, we show that vitamin A supplementation in the diet is also capable of inducing IL-18 in the gut, suggesting a dynamic regulation of epithelial IL-18 levels by dietary vitamin A.

In contrast to nutrient absorption and metabolism, which are well-studied, we know relatively little about the role of nutrient sensing in the epithelium. Specifically, our results highlight how vitamin A levels at homeostasis potentiate early epithelial-intrinsic and extrinsic communication during infection to mount an effective defense.

Our results demonstrate that IL-18 levels in the gut are transcriptionally regulated by vitamin A, however, the exact mechanism of this regulation remains unresolved. We hypothesize that vitamin A regulation of IL-18 occurs by an indirect mechanism involving an interplay between one or more direct targets of RAR signaling. Quantitative gene expression analysis has revealed a previously unknown interaction between RAR signaling, metallothioneins and intracellular labile zinc levels. A link between zinc and vitamin A has long been postulated, with correlations in the serum levels of both nutrients observed during disease states [58]. Vitamin A metabolic enzyme, retinol dehydrogenase, as well as retinoic acid receptor require zinc for their activity [59–61]. Our results suggest that this regulation might be bidirectional, with vitamin A signaling modulating zinc homeostasis in the epithelium. Unraveling how the epithelium integrates different nutritional cues to inform metabolism and immunity is crucial to understanding host response during infection.

Materials and methods

Mice

All mice were bred in the SPF barrier facility at Brown University. RAR403 is a dominant negative form of the retinoic acid receptor alpha. RAR403 lacks the carboxy terminal 59 amino acids of RARα, resulting in a truncated, 403 amino acid protein, incapable of responding to retinoic acid [62]. A construct containing RAR403 downstream of a loxP-flanked neomycin cassette was cloned in the Rosa26 locus, giving rise to $stop^{flox}$ mice [20]. Wild type $stop^{flox}$ mice were a kind gift from Dr. S. Sockanathan (Johns Hopkins University School of Medicine). Villin-Cre mice in a C56BL/6J background were purchased from Jackson Laboratories. $stop^{flox}$ mice were bred to Villin-Cre mice to get $stop^{flox}$ (Cre negative) or $stop^{\Delta IEC}$ (Cre positive) mice. All mice used in the study were 6–10 weeks old and were gender-matched across different groups. Littermates or co-housed mice were used to minimize microbiome mediated effects on the study.

Bacterial strains and maintenance

All infection experiments were carried out using *Salmonella* Typhimurium SL1344 GFP strain (kind gift of Dr. Vanessa Sperandio, UT Southwestern). Strain was routinely maintained on Luria Bertani agar plates containing 100 μg/ml ampicillin.

Mouse infections

For a gastroenteritis model of *Salmonella* infection protocol outlined by Barthel et al. was followed [23]. Briefly, mice were deprived of food and water for 4 hours and then orally gavaged with 20 mg streptomycin. After 20 hours, mice were again deprived of food and water for 4 hours. Overnight culture of *Salmonella* was subcultured for 4 hours, following which mice were infected with 10^8 bacteria by oral gavage. Mice were sacrificed 72 hours post infection to harvest organs and assess bacterial burden. For bacterial burden in distal colon, tissues were harvested, fileted and washed twice in phosphate-buffered saline (PBS). Tissues were then incubated in PBS containing 400 μg/ml gentamicin for 30 min at room temperature with shaking. Tissues were then rinsed with PBS, weighed, homogenized and plated to determine bacterial burden.

In order to assess the infection at early time points, protocol outlined by Sellin et al was followed [4]. The streptomycin treatment and *Salmonella* subculture was done as described above and mice were infected with $5x10^7$ bacteria by oral gavage. Assessment of cell death as well as tissue burden were performed in the cecum and proximal colon respectively which are the primary sites infected at this early time point. For cell death assessment, cecal tissues were harvested and fixed in 4% paraformaldehyde/4% sucrose overnight. Fixed tissues were then saturated in PBS containing 20% sucrose, embedded in optimal cutting temperature (OCT) medium, frozen over dry ice and stored at -80˚C. Proximal colon tissues were washed and gentamycin-treated for assessment of bacterial burden.

For reconstitution experiments, mouse recombinant IFNγ (Sino Biological; Cat. #50709-MNAH) and mouse recombinant IL-18 (Sino Biological; Cat. # 50073-MNCE) were used. Since IFNγ production defect in $stop^{\Delta IEC}$ mice was observed only after infection, reconstitution was performed 0 hr and 48hr post infection with 10 μg recombinant IFNγ intraperitoneally. Since $stop^{\Delta IEC}$ mice had homeostatic deficiency in IL-18 production, they were reconstituted with 2.5 μg recombinant IL-18 intraperitoneally 24 hours before and 24 hours after infection. For the early time point experiments, $stop^{\Delta IEC}$ mice received a single dose of 5 μg recombinant IL-18 intraperitoneally 24 hours before infection or a single dose of 15 μg recombinant IFNγ intraperitoneally 0 hours post infection. For IL-18 neutralization, $stop^{flox}$ mice were injected 200 μg of IL-18 neutralizing antibody (YIGIF74-1G7, Bioxcell) daily for 3 days, prior to infection with *Salmonella* [52].

Colonic lamina propria lymphocyte isolation and analysis

Colonic lamina propria lymphocytes were isolated as described by Kim et al [63]. Briefly, colons were flushed to remove luminal content, fileted, cut into three pieces and stored in ice-cold PBS. Tissues were washed by vigorous shaking, followed by sequential 10 min digestions at 37˚C in HBSS containing 3% FCS, 1mM dithiothreitol and 30mM ethylene diamine tetraacetic acid (EDTA) and HBSS containing 3% FCS and 30mM EDTA. Tissues were vigorously shaken between treatments to dislodge epithelial cells. Lymphocytes were liberated from the lamina propria by digesting tissues in RPMI complete containing 40 μl/ml collagenase (Sigma-Aldrich, stock solution 5 mg/ml) and 5 μl/ml DNase (Sigma- Aldrich, stock solution 0.5 mg/ml) for one hour at 37˚C followed by vigorous shaking. Cells were strained through a 70 μm

filter and separated on a discontinuous 40%/80% Percoll (GE Healthcare) gradient. Cells at the interface were harvested and processed for flow cytometry analysis.

Flow cytometry analysis

Cells were stimulated for 4 hours at 37˚C in RPMI complete containing 1X cell stimulation cocktail (eBioscience) and protein transport inhibitor cocktail (eBioscience). Stimulated cells were harvested and stained for surface markers and viability for 30 min at room temperature. Samples were stained with viability dye APCef780 (ThermoFisher), CD45 evolve655 (ThermoFisher), CD4 BV785 (BioLegend), CD3 eF450 (ThermoFisher), CD8a BV605 (BioLegend), CD335 BV510 (BioLegend) and Gr-1 FITC (eBioscience). Following overnight fixation using the Fixation/Permeabilization solution (eBioscience Foxp3 Staining Buffer Set), cells were permeabilized and stained for cytokines IL-17A AF488 (eBioscience), IL-22 PE (eBioscience) and IFNγ PE (eBioscience). Cells were analyzed using the Aria IIIu cytometer and data was analyzed using the FlowJo software.

Laser capture microdissection

Intestinal tissues were flushed with PBS and OCT, embedded in OCT, frozen on dry ice and stored at -80˚C. Cryosections (10 μm thick) were stained with methyl green and eosin. Intestinal epithelial cells were selectively captured using the Arcturus Laser capture Microdissection system. RNA was isolated from IECs using the RNAqueous-Micro Total RNA kit (Ambion).

Quantitative real time PCR. Isolated LCM RNA was converted into cDNA using the iScript cDNA synthesis kit (BioRad). Whole tissue samples were homogenized, RNA was extracted using the PureLink RNA isolation kit (Life Technologies) and converted to cDNA using MMLV reverse transcriptase. Quantitative real time PCR was carried out using SYBR green master mix (Maxima). Expression was normalized using *gapdh* as a housekeeping gene. Details of primers are provided in Table 1.

RNA-seq analysis

Laser capture microdissection was used to isolate RNA from small intestinal epithelial cells of homeostatic $stop^{flox}$ and $stop^{\Delta IEC}$ mice. Isolated RNA quality was checked using Picochip kit on 2100 Agilent Bioanalyser. RNA was processed using the Ovation Mouse RNA-seq system (NuGen) to produce a cDNA library. RNA was sequenced on an Illumina platform (1x50bp reads) and data was analyzed using the Galaxy platform [64]. Briefly, RNA seq reads were analyzed using FastQC and aligned to the mouse genome using Bowtie2. Aligned reads were

Table 1. Primers used in this study.

Primers	
Gapdh forward	5' AACTTTGGCATTGTGGAAGG 3'
Gapdh reverse	5' ACACATTGGGGGTAGGAACA 3'
Il18 forward	*5' GCCTCAAACCTTCCAAATCA 3'*
Il18 reverse	*5' TGGATCCATTTCCTCAAAGG 3'*
Isx forward	*5' TTCCACTTCACCCATTACCC 3'*
Isx reverse	5' CTCTTCTCCTGCTTCCTCCA 3'
mt1 forward	5′-GCTGTGCCTGATGTGACGAA-3′
mt1 reverse	5′-AGGAAGACGCTGGGTTGGT-3′
RARa forward	5'-GAAAAAGAAGAAAGAGGCACCCAAGC-3'
RARa reverse	5'-AGGTCAATGTCCAGGGAGACTCGTTG-3'

https://doi.org/10.1371/journal.ppat.1008360.t001

subjected to differential gene expression analysis using CuffDiff. Top 50 upregulated and downregulated genes (p value < 0.05) were visualized using GraphPad Prism. Raw data is deposited in the NCBI GEO repository (GSE140518). Complete list of differentially regulated genes can be found in S1 Table.

Barrier function analysis

BrdU incorporation assay was used for assessment of barrier turnover. Mice were injected intraperitoneally with 1 mg of bromodeoxyuridine. Mice were sacrificed 2 hours and 24 hours post injection, distal colon tissues were fixed in methacarn fixative and embedded in paraffin blocks. Tissue sections (7 μm thick) were stained with anti-BrdU antibody (Novus Biologicals; #NBP2-14890) and visualized. For mucus staining, colon tissues samples were fixed in methacarn and embedded in paraffin blocks. Tissue sections (7 μm thick) were stained with alcian blue-periodic acid Schiff's reagent to analyze mucus thickness and goblet cell numbers in the crypt.

Retinoid quantification. Homeostatic, littermate, gender-matched, 6–10 weeks old stop^{flox} and stop$^{\Delta IEC}$ mice were used for retinoid analysis. Mice were sacrificed and whole colon was harvested in dark. Colon tissue was flushed with PBS, fileted, frozen on dry ice and stored at -80˚C. Tissues were processed for retinoid quantification as described previously [18].

Immunofluorescence staining and confocal microscopy

For visualization of cell shedding and intracellular bacterial loads, PFA-fixed, OCT-embedded samples of cecum and proximal colon were cryosectioned to 10 μm thickness. Sections were air dried, permeabilized with 0.5% Triton X-100 and blocked with 10% donor goat serum. Sections were stained with anti-Salmonella LPS (Difco; #DF2659-47-5), anti-Cleaved Caspase-3 (Cell Signaling; #9661S) and anti-Epcam (BioLegend; #118201) antibody. DAPI was used to counterstain nuclei. Tissues were visualized using the Olympus FV3000 microscope.

Western Blot

For analysis of protein levels specifically in intestinal epithelial cells, colons were harvested and flushed with PBS. The colon epithelial cells were lysed in situ with tissue protein extraction reagent (TPER, Thermo Fisher) containing protease inhibitor cocktail. After 5 min incubation, lysate was recovered, centrifuged at 10,000 g for 3 min to remove debris and stored at -80˚C [65]. Whole tissue lysates were obtained by homogenizing tissue samples in 500 μl of TPER containing protease inhibitors and incubating on ice for 20 min. Lysates were centrifuged as above and stored at -80˚C. Protein in the samples were quantified using the DC protein assay (BioRad) and approximately 50 μg of protein was loaded for SDS-PAGE. Prestained protein ladder (BioRad) was loaded as a reference. Proteins were transferred on to PVDF membranes and blocked with 4% bovine serum albumin in TBST buffer for one hour. Blots were stained overnight at 4˚C using primary antibodies against IL-18 (Abcam; #ab71495) followed by incubation with appropriate secondary HRP-conjugated antibodies. Beta-actin (Santa Cruz; #sc-47778-HRP) levels in the sample were used for normalization. Blots were analyzed using ImageJ software to calculate relative protein levels.

Dietary intervention

6–8 weeks old stop^{flox} mice were fed regular mouse chow coated with retinyl acetate (500 IU/g) or equivalent amount of vehicle control (corn oil) for 2 weeks. Chow intake was monitored to ensure both groups of mice consumed similar amounts. Mice were sacrificed and colon lysates were prepared to analyze IL-18 levels using western blot.

Intracellular labile zinc analysis

Homeostatic stop^{flox} and stop$^{\Delta IEC}$ mice were sacrificed and colon tissues were harvested. Colon was flushed with cold PBS and fileted. Colon tissues were washed in cold PBS 3 times and in dPBS twice (vortexing for 1min each time). Tissues were digested in HBSS containing 1mM EDTA and 1mM DTT for 30min at 30˚C with shaking. Tissues were vortexed for 1min and filtered through a 40 μm filter to obtain epithelial cell fraction. Epithelial cells were washed in HBSS (3 times) and resuspended in dPBS. Cells were stained withCD326 APC (EpCAM; ThermoFisher), CD45 evolve655 (ThermoFisher) and Zinpry-1 FITC (Cayman Chemical company) and analyzed by flow cytometry.

Microscope image acquisition

Image acquisition was performed on the Olympus FV3000 confocal microscope. Images were acquired using a 60X oil immersion lens. For intracellular bacterial data, images were acquired as a Z-stack. All images processing was performed using the Fiji software with an Olympus plugin. Channel color for DAPI was changed to greyscale post-processing. Original 16-bit stacks were converted into RGB format before exporting as a video.

16S rRNA sequencing and microbiome analysis

Library preparation and sequencing. PCR amplification was performed using the Phusion High-Fidelity DNA polymerase with primers designed to flank the V4/V5 region of the 16S rRNA gene. Samples were submitted to the Genomics and Sequencing Center at the University of Rhode Island for PrepX NGS library preparation. Amplicons were sequenced using the Illumina MiSeq platform, yielding paired-end, 250-base-pair reads.

Processing of sequenced data. DADA2 pipeline [66] was used in R (version 3.3.4) and truncated reads where average Phred scores <30. The RDP classifier algorithm with the RDP training set 14 was used to perform taxonomic assignment [67]. ASV table was imported into R using phyloseq package [68]. Bar plots were made by converting sample counts into percentages to account for variations in sampling depth and exported into Prism software (GraphPad). Principal Coordinates of Analysis (PCoA) plots were generated using phyloseq and normalized by converting counts into relative abundance. Distance matrices were generated using both weighted and unweighted UniFrac distance metrics [69].

Statistical analysis

Data shown represent means ± SEM. Data was plotted and analyzed using GraphPad Prism software. For comparison of two groups, Student's t test was employed with two tailed analysis. Comparison of two or more groups was performed using One-way ANOVA. Two-way ANOVA was used to compare gene expression across multiple groups.

Ethics statement

All experiments were approved by and carried out in accordance with the guidelines of the Institutional Animal Care and Use Committee at Brown University (Protocol # 1803000345).

Supporting information

S1 Fig. Homeostatic colon retinoid and barrier analysis. This figure compares the (A) Total RA (retinoic acid), ROL (retinol) and RE (retinyl ester) normalized per gram of colon tissue, (B) mucus thickness, (C) goblet cells/crypt, (D and E) epithelial turnover via BrdU incorporation at 2 h (D) and 25 h (E) post injection in homeostatic colons of stop^{flox} and stop$^{\Delta IEC}$

mice. (F) Gene expression of retinoic acid receptor alpha in colon whole tissue at early and late timepoints of infection.
(TIF)

S2 Fig. Homeostatic microbiome analysis. This figure analysis the fecal microbial communities in homeostatic stop^{flox} and stop$^{\Delta IEC}$ mice using (A) unweighted Unifrac, (B) weighted Unifrac and displays the (C) relative abundance of microbial communities at the Class level.
(TIF)

S3 Fig. Homeostatic colon lamina propria lymphocyte characterization. This figure describes the relative frequencies of (A) CD45+CD3+ cells, (B) CD45+CD3+ IFNγ+ cells, (C) CD45+CD3+IL17+ cells and (D) IL22+ cells in the colons of stop^{flox} and stop$^{\Delta IEC}$ mice at homeostasis.
(TIF)

S4 Fig. Colon lamina propria lymphocyte characterization during infection. This figure describes the relative frequencies of (A) CD4 and CD8 cells, (B) Gr-1+ cells, (C) CD3+ IL17+ and (D) CD45+IL22+ cells in colonic lamina propria of stop^{flox} and stop$^{\Delta IEC}$ mice 72 hours post *Salmonella* infection.
(TIF)

S5 Fig. RNAseq analysis. This figure compares gene expression in laser capture microdissected epithelial cells from ileal tissues of homeostatic stop^{flox} and stop$^{\Delta IEC}$ mice. (A) Volcano plot displaying global changes in gene expression. (B) Heat map detailing top 50 downregulated and upregulated genes. (C) Relative expression of *mt1* gene in ileal epithelial cells (D and E) Flow cytometry analysis of EpCAM+ colon epithelial cells from homeostatic stop^{flox} and stop$^{\Delta IEC}$ mice and quantitative analysis of cellular Zinpyr-1 fluorescence.
(TIF)

S6 Fig. Colon lamina propria lymphocyte characterization at 18 hours post infection. This figure describes the relative frequencies of IFNγ+ cells in colonic lamina propria of stop^{flox} and stop$^{\Delta IEC}$ mice 18 hours post *Salmonella* infection.
(TIF)

S7 Fig. IL-18 neutralization experiment. This figure compares epithelial cell shedding at 18 hpi in (A) control and (B) anti-IL18 treated mice with (C) quantitative analysis.
(TIF)

S1 Movie. Intracellular *Salmonella* burden in stop^{flox} mice. Video of Z stacks imaging for intracellular loads of *Salmonella* in proximal colon tissues of stop^{flox} mice at 18 hours post infection.
(MOV)

S2 Movie. Intracellular *Salmonella* burden in stop$^{\Delta IEC}$ mice. Video of Z stacks imaging for intracellular loads of *Salmonella* in proximal colon tissues of stop$^{\Delta IEC}$ mice at 18 hours post infection.
(MOV)

S3 Movie. Intracellular *Salmonella* burden in stop$^{\Delta IEC}$ + IL-18 mice. Video of Z stacks imaging for intracellular loads of *Salmonella* in proximal colon tissues of stop$^{\Delta IEC}$ + IL-18 mice at 18 hours post infection.
(MOV)

S1 Table. Complete list of differentially regulated genes from RNAseq analysis of IECs from $stop^{flox}$ and $stop^{\Delta IEC}$ mice at homeostasis.
(XLSX)

Acknowledgments

We thank Kevin Carlson for assistance with flow cytometry and Geoff Williams for maintaining the Leduc Bioimaging facility. We thank Christoph Schorl and the Brown Genomics core for help with the RNA sequencing.

Author Contributions

Conceptualization: Namrata Iyer, Shipra Vaishnava.

Data curation: Namrata Iyer, Shipra Vaishnava.

Formal analysis: Namrata Iyer, Shipra Vaishnava.

Funding acquisition: Namrata Iyer, Shipra Vaishnava.

Investigation: Namrata Iyer, Mayara Grizotte-Lake, Kellyanne Duncan, Sarah R. Gordon, Guo Zhong.

Methodology: Namrata Iyer, Kellyanne Duncan, Guo Zhong, Nina Isoherranen.

Project administration: Shipra Vaishnava.

Resources: Ana C. S. Palmer.

Supervision: Shipra Vaishnava.

Validation: Namrata Iyer, Crystle Calvin.

Writing – original draft: Namrata Iyer, Shipra Vaishnava.

Writing – review & editing: Namrata Iyer, Shipra Vaishnava.

References

1. Allaire JM, Crowley SM, Law HT, Chang SY, Ko HJ, Vallance BA. The Intestinal Epithelium: Central Coordinator of Mucosal Immunity. Trends Immunol. 2018; 39(9):677–96. https://doi.org/10.1016/j.it.2018.04.002 PMID: 29716793.
2. Thiemann S, Smit N, Roy U, Lesker TR, Galvez EJC, Helmecke J, et al. Enhancement of IFNgamma Production by Distinct Commensals Ameliorates Salmonella-Induced Disease. Cell Host Microbe. 2017; 21(6):682–94 e5. https://doi.org/10.1016/j.chom.2017.05.005 PMID: 28618267.
3. Muller AA, Dolowschiak T, Sellin ME, Felmy B, Verbree C, Gadient S, et al. An NK Cell Perforin Response Elicited via IL-18 Controls Mucosal Inflammation Kinetics during Salmonella Gut Infection. PLoS Pathog. 2016; 12(6):e1005723. https://doi.org/10.1371/journal.ppat.1005723 PMID: 27341123; PubMed Central PMCID: PMC4920399.
4. Sellin ME, Muller AA, Felmy B, Dolowschiak T, Diard M, Tardivel A, et al. Epithelium-intrinsic NAIP/NLRC4 inflammasome drives infected enterocyte expulsion to restrict Salmonella replication in the intestinal mucosa. Cell Host Microbe. 2014; 16(2):237–48. https://doi.org/10.1016/j.chom.2014.07.001 PMID: 25121751.
5. Liu J, Bolick DT, Kolling GL, Fu Z, Guerrant RL. Protein Malnutrition Impairs Intestinal Epithelial Cell Turnover, a Potential Mechanism of Increased Cryptosporidiosis in a Murine Model. Infect Immun. 2016; 84(12):3542–9. https://doi.org/10.1128/IAI.00705-16 PMID: 27736783; PubMed Central PMCID: PMC5116730.
6. Harrison EH. Mechanisms involved in the intestinal absorption of dietary vitamin A and provitamin A carotenoids. Biochim Biophys Acta. 2012; 1821(1):70–7. https://doi.org/10.1016/j.bbalip.2011.06.002 PMID: 21718801; PubMed Central PMCID: PMC3525326.

7. Coombes JL, Siddiqui KR, Arancibia-Carcamo CV, Hall J, Sun CM, Belkaid Y, et al. A functionally specialized population of mucosal CD103+ DCs induces Foxp3+ regulatory T cells via a TGF-beta and retinoic acid-dependent mechanism. J Exp Med. 2007; 204(8):1757–64. https://doi.org/10.1084/jem.20070590 PMID: 17620361; PubMed Central PMCID: PMC2118683.

8. Hall JA, Cannons JL, Grainger JR, Dos Santos LM, Hand TW, Naik S, et al. Essential role for retinoic acid in the promotion of CD4(+) T cell effector responses via retinoic acid receptor alpha. Immunity. 2011; 34(3):435–47. https://doi.org/10.1016/j.immuni.2011.03.003 PMID: 21419664; PubMed Central PMCID: PMC3415227.

9. Mora JR, von Andrian UH. Role of retinoic acid in the imprinting of gut-homing IgA-secreting cells. Semin Immunol. 2009; 21(1):28–35. https://doi.org/10.1016/j.smim.2008.08.002 PMID: 18804386; PubMed Central PMCID: PMC2663412.

10. Goverse G, Labao-Almeida C, Ferreira M, Molenaar R, Wahlen S, Konijn T, et al. Vitamin A Controls the Presence of RORgamma+ Innate Lymphoid Cells and Lymphoid Tissue in the Small Intestine. J Immunol. 2016; 196(12):5148–55. https://doi.org/10.4049/jimmunol.1501106 PMID: 27183576.

11. Jijon HB, Suarez-Lopez L, Diaz OE, Das S, De Calisto J, Parada-Kusz M, et al. Correction: Intestinal epithelial cell-specific RARalpha depletion results in aberrant epithelial cell homeostasis and underdeveloped immune system. Mucosal Immunol. 2019; 12(2):580. https://doi.org/10.1038/s41385-018-0074-8 PMID: 30514887.

12. Gattu S, Bang YJ, Pendse M, Dende C, Chara AL, Harris TA, et al. Epithelial retinoic acid receptor beta regulates serum amyloid A expression and vitamin A-dependent intestinal immunity. Proc Natl Acad Sci U S A. 2019. https://doi.org/10.1073/pnas.1812069116 PMID: 31097581.

13. McClung L, Winters J. Effect of Vitamin A-Free Diet on Resistance to Infection by Salmonella enteritidis. The Journal of Infectious Diseases. 1932; 51(3):469–74

14. Imdad A, Mayo-Wilson E, Herzer K, Bhutta ZA. Vitamin A supplementation for preventing morbidity and mortality in children from six months to five years of age. Cochrane Database Syst Rev. 2017; 3: CD008524. https://doi.org/10.1002/14651858.CD008524.pub3 PMID: 28282701; PubMed Central PMCID: PMC6464706.

15. Huang Z, Liu Y, Qi G, Brand D, Zheng SG. Role of Vitamin A in the Immune System. J Clin Med. 2018; 7(9). https://doi.org/10.3390/jcm7090258 PMID: 30200565; PubMed Central PMCID: PMC6162863.

16. Villamor E, Fawzi WW. Effects of vitamin a supplementation on immune responses and correlation with clinical outcomes. Clin Microbiol Rev. 2005; 18(3):446–64. https://doi.org/10.1128/CMR.18.3.446-464.2005 PMID: 16020684; PubMed Central PMCID: PMC1195969.

17. Das BC, Thapa P, Karki R, Das S, Mahapatra S, Liu TC, et al. Retinoic acid signaling pathways in development and diseases. Bioorg Med Chem. 2014; 22(2):673–83. https://doi.org/10.1016/j.bmc.2013.11.025 PMID: 24393720; PubMed Central PMCID: PMC4447240.

18. Grizotte-Lake M, Zhong G, Duncan K, Kirkwood J, Iyer N, Smolenski I, et al. Commensals Suppress Intestinal Epithelial Cell Retinoic Acid Synthesis to Regulate Interleukin-22 Activity and Prevent Microbial Dysbiosis. Immunity. 2018; 49(6):1103–15 e6. https://doi.org/10.1016/j.immuni.2018.11.018 PMID: 30566883; PubMed Central PMCID: PMC6319961.

19. Iliev ID, Mileti E, Matteoli G, Chieppa M, Rescigno M. Intestinal epithelial cells promote colitis-protective regulatory T-cell differentiation through dendritic cell conditioning. Mucosal Immunol. 2009; 2(4):340–50. https://doi.org/10.1038/mi.2009.13 PMID: 19387433.

20. Rajaii F, Bitzer ZT, Xu Q, Sockanathan S. Expression of the dominant negative retinoid receptor, RAR403, alters telencephalic progenitor proliferation, survival, and cell fate specification. Dev Biol. 2008; 316(2):371–82. https://doi.org/10.1016/j.ydbio.2008.01.041 PMID: 18329011.

21. Tsai S, Bartelmez S, Heyman R, Damm K, Evans R, Collins SJ. A mutated retinoic acid receptor-alpha exhibiting dominant-negative activity alters the lineage development of a multipotent hematopoietic cell line. Genes Dev. 1992; 6(12A):2258–69. https://doi.org/10.1101/gad.6.12a.2258 PMID: 1334022.

22. Lobo GP, Hessel S, Eichinger A, Noy N, Moise AR, Wyss A, et al. ISX is a retinoic acid-sensitive gatekeeper that controls intestinal beta,beta-carotene absorption and vitamin A production. FASEB J. 2010; 24(6):1656–66. https://doi.org/10.1096/fj.09-150995 PMID: 20061533; PubMed Central PMCID: PMC2874479.

23. Barthel M, Hapfelmeier S, Quintanilla-Martinez L, Kremer M, Rohde M, Hogardt M, et al. Pretreatment of mice with streptomycin provides a Salmonella enterica serovar Typhimurium colitis model that allows analysis of both pathogen and host. Infect Immun. 2003; 71(5):2839–58. https://doi.org/10.1128/IAI.71.5.2839-2858.2003 PMID: 12704158; PubMed Central PMCID: PMC153285.

24. Iwata M, Eshima Y, Kagechika H. Retinoic acids exert direct effects on T cells to suppress Th1 development and enhance Th2 development via retinoic acid receptors. Int Immunol. 2003; 15(8):1017–25. https://doi.org/10.1093/intimm/dxg101 PMID: 12882839.

25. Brown CC, Esterhazy D, Sarde A, London M, Pullabhatla V, Osma-Garcia I, et al. Retinoic acid is essential for Th1 cell lineage stability and prevents transition to a Th17 cell program. Immunity. 2015; 42(3):499–511. https://doi.org/10.1016/j.immuni.2015.02.003 PMID: 25769610; PubMed Central PMCID: PMC4372260.

26. Mielke LA, Jones SA, Raverdeau M, Higgs R, Stefanska A, Groom JR, et al. Retinoic acid expression associates with enhanced IL-22 production by gammadelta T cells and innate lymphoid cells and attenuation of intestinal inflammation. J Exp Med. 2013; 210(6):1117–24. https://doi.org/10.1084/jem.20121588 PMID: 23690441; PubMed Central PMCID: PMC3674702.

27. Rampal R, Awasthi A, Ahuja V. Retinoic acid-primed human dendritic cells inhibit Th9 cells and induce Th1/Th17 cell differentiation. J Leukoc Biol. 2016; 100(1):111–20. https://doi.org/10.1189/jlb.3VMA1015-476R PMID: 26980802.

28. Bao S, Beagley KW, France MP, Shen J, Husband AJ. Interferon-gamma plays a critical role in intestinal immunity against Salmonella typhimurium infection. Immunology. 2000; 99(3):464–72. https://doi.org/10.1046/j.1365-2567.2000.00955.x PMID: 10712678; PubMed Central PMCID: PMC2327174.

29. Gordon MA, Jack DL, Dockrell DH, Lee ME, Read RC. Gamma interferon enhances internalization and early nonoxidative killing of Salmonella enterica serovar Typhimurium by human macrophages and modifies cytokine responses. Infect Immun. 2005; 73(6):3445–52. https://doi.org/10.1128/IAI.73.6.3445-3452.2005 PMID: 15908373; PubMed Central PMCID: PMC1111838.

30. Dinarello CA, Novick D, Kim S, Kaplanski G. Interleukin-18 and IL-18 binding protein. Front Immunol. 2013; 4:289. https://doi.org/10.3389/fimmu.2013.00289 PMID: 24115947; PubMed Central PMCID: PMC3792554.

31. Yoshimoto T, Takeda K, Tanaka T, Ohkusu K, Kashiwamura S, Okamura H, et al. IL-12 up-regulates IL-18 receptor expression on T cells, Th1 cells, and B cells: synergism with IL-18 for IFN-gamma production. J Immunol. 1998; 161(7):3400–7. PMID: 9759857.

32. Kolinska J, Lisa V, Clark JA, Kozakova H, Zakostelecka M, Khailova L, et al. Constitutive expression of IL-18 and IL-18R in differentiated IEC-6 cells: effect of TNF-alpha and IFN-gamma treatment. J Interferon Cytokine Res. 2008; 28(5):287–96. https://doi.org/10.1089/jir.2006.0130 PMID: 18547159.

33. Pizarro TT, Michie MH, Bentz M, Woraratanadharm J, Smith MF Jr, Foley E, et al. IL-18, a novel immunoregulatory cytokine, is up-regulated in Crohn's disease: expression and localization in intestinal mucosal cells. J Immunol. 1999; 162(11):6829–35. PMID: 10352304.

34. Sallmon H, Hoene V, Weber SC, Dame C. Differentiation of human SH-SY5Y neuroblastoma cells by all-trans retinoic acid activates the interleukin-18 system. J Interferon Cytokine Res. 2010; 30(2):55–8. https://doi.org/10.1089/jir.2009.0036 PMID: 20028206.

35. Gushchina LV, Yasmeen R, Ziouzenkova O. Moderate vitamin A supplementation in obese mice regulates tissue factor and cytokine production in a sex-specific manner. Arch Biochem Biophys. 2013; 539(2):239–47. https://doi.org/10.1016/j.abb.2013.06.020 PMID: 23850584; PubMed Central PMCID: PMC3818464.

36. Lalevee S, Anno YN, Chatagnon A, Samarut E, Poch O, Laudet V, et al. Genome-wide in silico identification of new conserved and functional retinoic acid receptor response elements (direct repeats separated by 5 bp). J Biol Chem. 2011; 286(38):33322–34. https://doi.org/10.1074/jbc.M111.263681 PMID: 21803772; PubMed Central PMCID: PMC3190930.

37. Delacroix L, Moutier E, Altobelli G, Legras S, Poch O, Choukrallah MA, et al. Cell-specific interaction of retinoic acid receptors with target genes in mouse embryonic fibroblasts and embryonic stem cells. Mol Cell Biol. 2010; 30(1):231–44. https://doi.org/10.1128/MCB.00756-09 PMID: 19884340; PubMed Central PMCID: PMC2798310.

38. Yasuda K, Nakanishi K, Tsutsui H. Interleukin-18 in Health and Disease. Int J Mol Sci. 2019; 20(3). https://doi.org/10.3390/ijms20030649 PMID: 30717382; PubMed Central PMCID: PMC6387150.

39. Zhu Q, Kanneganti TD. Cutting Edge: Distinct Regulatory Mechanisms Control Proinflammatory Cytokines IL-18 and IL-1beta. J Immunol. 2017; 198(11):4210–5. https://doi.org/10.4049/jimmunol.1700352 PMID: 28468974; PubMed Central PMCID: PMC5544497.

40. Takeda N, Arima M, Tsuruoka N, Okada S, Hatano M, Sakamoto A, et al. Bcl6 is a transcriptional repressor for the IL-18 gene. J Immunol. 2003; 171(1):426–31. https://doi.org/10.4049/jimmunol.171.1.426 PMID: 12817026.

41. Krezel A, Maret W. The Functions of Metamorphic Metallothioneins in Zinc and Copper Metabolism. Int J Mol Sci. 2017; 18(6). https://doi.org/10.3390/ijms18061237 PMID: 28598392; PubMed Central PMCID: PMC5486060.

42. Ruttkay-Nedecky B, Nejdl L, Gumulec J, Zitka O, Masarik M, Eckschlager T, et al. The role of metallothionein in oxidative stress. Int J Mol Sci. 2013; 14(3):6044–66. https://doi.org/10.3390/ijms14036044 PMID: 23502468; PubMed Central PMCID: PMC3634463.

43. Kagi JH. Overview of metallothionein. Methods Enzymol. 1991; 205:613–26. https://doi.org/10.1016/0076-6879(91)05145-l PMID: 1779825.

44. Woodroofe CC, Masalha R, Barnes KR, Frederickson CJ, Lippard SJ. Membrane-permeable and -impermeable sensors of the Zinpyr family and their application to imaging of hippocampal zinc in vivo. Chem Biol. 2004; 11(12):1659–66. https://doi.org/10.1016/j.chembiol.2004.09.013 PMID: 15610850.

45. Uzzo RG, Crispen PL, Golovine K, Makhov P, Horwitz EM, Kolenko VM. Diverse effects of zinc on NF-kappaB and AP-1 transcription factors: implications for prostate cancer progression. Carcinogenesis. 2006; 27(10):1980–90. https://doi.org/10.1093/carcin/bgl034 PMID: 16606632.

46. Thiennimitr P, Winter SE, Winter MG, Xavier MN, Tolstikov V, Huseby DL, et al. Intestinal inflammation allows Salmonella to use ethanolamine to compete with the microbiota. Proc Natl Acad Sci U S A. 2011; 108(42):17480–5. https://doi.org/10.1073/pnas.1107857108 PMID: 21969563; PubMed Central PMCID: PMC3198331.

47. Winter SE, Thiennimitr P, Winter MG, Butler BP, Huseby DL, Crawford RW, et al. Gut inflammation provides a respiratory electron acceptor for Salmonella. Nature. 2010; 467(7314):426–9. https://doi.org/10.1038/nature09415 PMID: 20864996; PubMed Central PMCID: PMC2946174.

48. Rauch I, Deets KA, Ji DX, von Moltke J, Tenthorey JL, Lee AY, et al. NAIP-NLRC4 Inflammasomes Coordinate Intestinal Epithelial Cell Expulsion with Eicosanoid and IL-18 Release via Activation of Caspase-1 and -8. Immunity. 2017; 46(4):649–59. https://doi.org/10.1016/j.immuni.2017.03.016 PMID: 28410991; PubMed Central PMCID: PMC5476318.

49. Williams JM, Duckworth CA, Burkitt MD, Watson AJ, Campbell BJ, Pritchard DM. Epithelial cell shedding and barrier function: a matter of life and death at the small intestinal villus tip. Vet Pathol. 2015; 52(3):445–55. https://doi.org/10.1177/0300985814559404 PMID: 25428410; PubMed Central PMCID: PMC4441880.

50. Knodler LA, Crowley SM, Sham HP, Yang H, Wrande M, Ma C, et al. Noncanonical inflammasome activation of caspase-4/caspase-11 mediates epithelial defenses against enteric bacterial pathogens. Cell Host Microbe. 2014; 16(2):249–56. https://doi.org/10.1016/j.chom.2014.07.002 PMID: 25121752; PubMed Central PMCID: PMC4157630.

51. Navabi N, Whitt J, Wu SE, Woo V, Moncivaiz J, Jordan MB, et al. Epithelial Histone Deacetylase 3 Instructs Intestinal Immunity by Coordinating Local Lymphocyte Activation. Cell Rep. 2017; 19(6):1165–75. https://doi.org/10.1016/j.celrep.2017.04.046 PMID: 28494866; PubMed Central PMCID: PMC5499685.

52. Chudnovskiy A, Mortha A, Kana V, Kennard A, Ramirez JD, Rahman A, et al. Host-Protozoan Interactions Protect from Mucosal Infections through Activation of the Inflammasome. Cell. 2016; 167(2):444–56 e14. https://doi.org/10.1016/j.cell.2016.08.076 PMID: 27716507; PubMed Central PMCID: PMC5129837.

53. Bono MR, Tejon G, Flores-Santibanez F, Fernandez D, Rosemblatt M, Sauma D. Retinoic Acid as a Modulator of T Cell Immunity. Nutrients. 2016; 8(6). https://doi.org/10.3390/nu8060349 PMID: 27304965; PubMed Central PMCID: PMC4924190.

54. Tone M, Thompson SA, Tone Y, Fairchild PJ, Waldmann H. Regulation of IL-18 (IFN-gamma-inducing factor) gene expression. J Immunol. 1997; 159(12):6156–63. PMID: 9550417.

55. Kempster SL, Belteki G, Forhead AJ, Fowden AL, Catalano RD, Lam BY, et al. Developmental control of the Nlrp6 inflammasome and a substrate, IL-18, in mammalian intestine. Am J Physiol Gastrointest Liver Physiol. 2011; 300(2):G253–63. https://doi.org/10.1152/ajpgi.00397.2010 PMID: 21088234; PubMed Central PMCID: PMC3043648.

56. Levy M, Thaiss CA, Zeevi D, Dohnalova L, Zilberman-Schapira G, Mahdi JA, et al. Microbiota-Modulated Metabolites Shape the Intestinal Microenvironment by Regulating NLRP6 Inflammasome Signaling. Cell. 2015; 163(6):1428–43. https://doi.org/10.1016/j.cell.2015.10.048 PMID: 26638072.

57. Kalina U, Koyama N, Hosoda T, Nuernberger H, Sato K, Hoelzer D, et al. Enhanced production of IL-18 in butyrate-treated intestinal epithelium by stimulation of the proximal promoter region. Eur J Immunol. 2002; 32(9):2635–43. https://doi.org/10.1002/1521-4141(200209)32:9<2635::AID-IMMU2635>3.0.CO;2-N PMID: 12207348.

58. Smith JC Jr., McDaniel EG, Fan FF, Halsted JA. Zinc: a trace element essential in vitamin A metabolism. Science. 1973; 181(4103):954–5. https://doi.org/10.1126/science.181.4103.954 PMID: 4730448.

59. Morris DR, Levenson CW. Zinc regulation of transcriptional activity during retinoic acid-induced neuronal differentiation. J Nutr Biochem. 2013; 24(11):1940–4. https://doi.org/10.1016/j.jnutbio.2013.06.002 PMID: 24029070; PubMed Central PMCID: PMC3832953.

60. Casadevall M, Sarkar B. Effect of redox conditions on the DNA-binding efficiency of the retinoic acid receptor zinc-finger. J Inorg Biochem. 1998; 71(3–4):147–52. PMID: 9833319.

61. Christian P, West KP Jr. Interactions between zinc and vitamin A: an update. Am J Clin Nutr. 1998; 68(2 Suppl):435S–41S. https://doi.org/10.1093/ajcn/68.2.435S PMID: 9701158.

62. Damm K, Heyman RA, Umesono K, Evans RM. Functional inhibition of retinoic acid response by dominant negative retinoic acid receptor mutants. Proc Natl Acad Sci U S A. 1993; 90(7):2989–93. https://doi.org/10.1073/pnas.90.7.2989 PMID: 8096643; PubMed Central PMCID: PMC46222.

63. Kim M, Galan C, Hill AA, Wu WJ, Fehlner-Peach H, Song HW, et al. Critical Role for the Microbiota in CX3CR1(+) Intestinal Mononuclear Phagocyte Regulation of Intestinal T Cell Responses. Immunity. 2018; 49(1):151–63 e5. https://doi.org/10.1016/j.immuni.2018.05.009 PMID: 29980437; PubMed Central PMCID: PMC6051886.

64. Afgan E, Baker D, Batut B, van den Beek M, Bouvier D, Cech M, et al. The Galaxy platform for accessible, reproducible and collaborative biomedical analyses: 2018 update. Nucleic Acids Res. 2018; 46 (W1):W537–W44. https://doi.org/10.1093/nar/gky379 PMID: 29790989; PubMed Central PMCID: PMC6030816.

65. Benjamin JL, Sumpter R Jr., Levine B, Hooper LV. Intestinal epithelial autophagy is essential for host defense against invasive bacteria. Cell Host Microbe. 2013; 13(6):723–34. https://doi.org/10.1016/j.chom.2013.05.004 PMID: 23768496; PubMed Central PMCID: PMC3755484.

66. Callahan BJ, McMurdie PJ, Rosen MJ, Han AW, Johnson AJ, Holmes SP. DADA2: High-resolution sample inference from Illumina amplicon data. Nat Methods. 2016; 13(7):581–3. Epub 2016/05/24. https://doi.org/10.1038/nmeth.3869 PMID: 27214047; PubMed Central PMCID: PMC4927377.

67. Wang Q, Garrity GM, Tiedje JM, Cole JR. Naive Bayesian classifier for rapid assignment of rRNA sequences into the new bacterial taxonomy. Applied and environmental microbiology. 2007; 73 (16):5261–7. Epub 2007/06/22. https://doi.org/10.1128/AEM.00062-07 PMID: 17586664.

68. McMurdie PJ, Holmes S. phyloseq: an R package for reproducible interactive analysis and graphics of microbiome census data. PLoS One. 2013; 8(4):e61217. Epub 2013/05/01. https://doi.org/10.1371/journal.pone.0061217 PMID: 23630581; PubMed Central PMCID: PMC3632530.

69. Lozupone C, Knight R. UniFrac: a new phylogenetic method for comparing microbial communities. Appl Environ Microbiol. 2005; 71(12):8228–35. Epub 2005/12/08. https://doi.org/10.1128/AEM.71.12.8228-8235.2005 PMID: 16332807; PubMed Central PMCID: PMC1317376.